Numerical investigation and actuator design for Advanced Digital Sound Reconstruction

Dominik Mayrhofer[1], Manfred Kaltenbacher[2]

[1] Institue of Fundamentals and Theory in Electrical Engineering, 8010 Graz, Austria, Email: dominik.mayrhofer@tugraz.at

[2] Institue of Fundamentals and Theory in Electrical Engineering, 8010 Graz, Austria, Email: manfred.kaltenbacher@tugraz.at

Abstract

The actuator design for a new method of sound generation – which we call Advanced Digital Sound Reconstruction (ADSR) – is a very challenging task due to the increased complexity of the actuator compared to a standard loudspeaker. The basic principle of ADSR relies on the generation of purely positive or negative sound pulses, which can be achieved by equipping a membrane with shutter gates. Combining multiple of these actuators and superimposing the sound pulses enables the generation of an audio signal. The actuator itself is designed as a Micro-Electro-Mechanical-Systems (MEMS) device since ADSR requires a highly dynamic actuator. Due to the small scale, viscous effects have to be taken into account. Furthermore, the shutter gates used for the separation of sound pulses introduce additional sound emissions which have to be mitigated. Based on these challenges, numerical investigations using the linearized flow equations in order to solve for the acoustic pressure have been performed. We present studies on the influence of different parameters on the acoustic transmission properties of the actuator in order to optimize the system. The results of the parameter study are finally translated to design guidelines in order to aid in the early design stages.

Introduction

Based on the initial idea of Digital Sound Reconstruction (DSR) [1], a new method for sound generation called Advanced Digital Sound Reconstruction has been introduced in [2, 3]. Besides the already known concept of superimposing multiple sound pressure pulses to form an audio signal, this new concept utilizes a shutter mechanism to redirect sound pulses depending on their sign. Hence, the actuator used for this principle can generate purely positive or negative sound pulses in a channel which can be used for the superposition process. The main advantage of this approach is that the sound pressure does not follow the classical scaling laws (e.g. linear scaling with the frequency in an infinite channel), but one order lower. Hence, for the infinite channel, this results in a constant sound pressure level over the frequency. In an ear-coupler, the sound pressure scales with $1/f$ for low frequencies, leading to a large benefit regarding achievable sound pressure levels with respect to a standard loudspeaker. The smallest unit for ADSR producing this sound pressure pulses consists of a membrane and two shutters and will be denoted as a Unit Cell (UC). Due to the high frequency content, extra care has to be taken when designing such a UC with respect to its acoustic properties. The design of such a UC – especially for Micro-Electro-Mechanical-Systems (MEMS) applications – has not yet been investigated thoroughly. Hence, an underlying study of the geometry has been carried out which gives general guidance for the design process.

Governing equations

For the numerical investigations two physical fields have been considered in the frequency domain. First of all, the classic acoustic wave equation

$$\frac{\omega^2}{c_0^2}\underline{p}_\mathrm{a} + \nabla \cdot \nabla \underline{p}_\mathrm{a} = 0 \tag{1}$$

has been used in regions where viscous effects are negligible. In this equation, ω represents the angular frequency, c_0 the speed of sound and $\underline{p}_\mathrm{a}$ the (complex) acoustic sound pressure. Since we are dealing with MEMS structures, the valve itself exhibits very narrow slits where the acoustic wave has to pass through. Hence, these narrow passages require a more sophisticated modeling approach. Therefore, we utilize the linearized flow (LF) equations which can be derived from the compressible flow equations by using a perturbation ansatz and neglecting second order terms. The resulting system of equations is given by

$$j\omega\rho_0\underline{\boldsymbol{v}} - \nabla \cdot \underline{\boldsymbol{\sigma}} = 0 \tag{2}$$

$$\underline{\boldsymbol{\sigma}} = -\underline{p}\boldsymbol{I} + \mu\left(\nabla\underline{\boldsymbol{v}} + (\nabla\underline{\boldsymbol{v}})^\mathsf{T}\right) + \left(\lambda_\mathrm{f} - \frac{2}{3}\mu\right)(\nabla \cdot \underline{\boldsymbol{v}})\,\boldsymbol{I} \tag{3}$$

$$\frac{j\omega}{\rho_0 c_0^2}\,\underline{p} + \nabla \cdot \underline{\boldsymbol{v}} = 0. \tag{4}$$

In these equations ρ_0 denotes the mean density, $\underline{\boldsymbol{v}}$ the perturbed fluid velocity and $\underline{\boldsymbol{\sigma}}$ the viscous stress tensor. Furthermore, $\underline{p}$ represents the perturbed fluid pressure, $\boldsymbol{I}$ the identity matrix, μ the dynamic viscosity and λ_f the volume viscosity. With equations (2)-(4) we include the viscous losses caused by the narrow slits while saving computation time by coupling them to (1). This coupling can be achieved by using the continuity of surface traction

$$-\underline{p}_\mathrm{a}\boldsymbol{n} = \underline{\boldsymbol{\sigma}} \cdot \boldsymbol{n} \tag{5}$$

as well as the continuity of the normal acceleration

$$j\omega\,\underline{\boldsymbol{v}} \cdot \boldsymbol{n} = -\frac{1}{\rho_0}\nabla\underline{p}_\mathrm{a} \cdot \boldsymbol{n}. \tag{6}$$

Here $\boldsymbol{n}$ denotes the outward facing normal vector as seen from the domain used for the linearized flow equations. For the boundary conditions the LF-domain has been mostly enclosed with a no-slip boundary condition except for the coupling- and symmetry surfaces. Since we utilize symmetries of the model, we have to enforce it via a surface mass which is similar to a normal traction proportional to the normal velocity. Regarding the excitation, the acoustic particle velocity in normal direction is prescribed at the speaker surface as

$$\underline{v}_\mathrm{n} = \underline{\boldsymbol{v}}_\mathrm{a} \cdot \boldsymbol{n} = s_\mathrm{a}\,\omega\,\frac{d_\mathrm{V}^2}{d_\mathrm{BV}^2}. \tag{7}$$

In this equation $\underline{v}_\mathrm{n}$ represents the normal velocity at the boundary, s_a the displacement amplitude of 300 nm, d_V the diameter of the valve and d_BV the diameter of the back volume. The scaling factor $d_\mathrm{V}^2/d_\mathrm{BV}^2$ is used to adjust the resulting sound pressure. Using a simplified plane wave model, this scaling would result in a similar sound pressure for all the different geometries at the observation point which makes the comparison easier.

Model setup

The main focus of this work was to investigate the interaction between the front shutter and the membrane responsible for sound generation. We have chosen an embodiment based on a classical electrostatic membrane combined with a valve mechanism based on the same principle. The general structure of this valve can be seen in Fig. 1 and is similar to the one presented in [4] – only with adapted geometry.

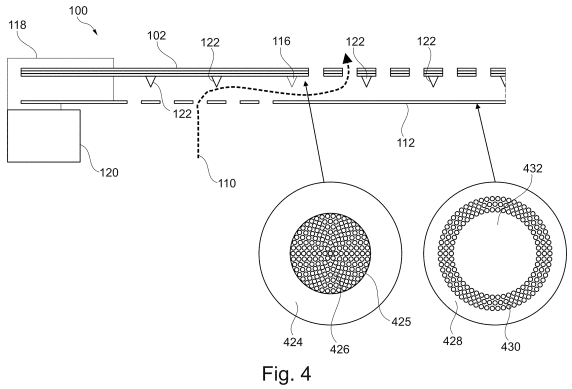

Figure 1: Structure of the valve [4].

As it can be seen, the top back plate (TBP) and the bottom back plate (BBP) are inversely perforated in order to have a low impedance in the open state while effectively sealing the channel in the closed state. We investigated different sizes of the volume between the speaker and valve, which we denote as back volume (BV) in this case, since it is the back volume from the valves perspective. Regarding the geometry, the dimensions used for the simulation can be seen in Tab. 1.

It has to be noted, that the perforation of the BBP has been chosen equally to the one of the TBP for the model, but for the actual simulations, the reduced perforation

Table 1: Geometry of the valve

Parameter	Value
Valve diameter d_V	0.5 mm
Thickness TBP h_TBP	1 µm
Thickness BBP h_BBP	1 µm
Gap height h_gap	4 µm
Perforation TBP	36.5 %
Perforation BBP	36.5 % / 28 %
Hole diameter d_h	10 µm
BV diameter d_BV	0.9 mm - 10 mm
BV height h_BV	0.2 mm - 1 mm

grade of 28 % has been used. The reason for this is the exclusion of the outer most ring for the simulation which accounts for the region used for clamping. The holes are automatically generated during the model generation process, however, for a more realistic approach they have been excluded for the simulations. The effect of including and excluding the outer most ring has been studied in an extra acoustic simulation and has been determined to be negligible, as it can be seen in Fig. 2.

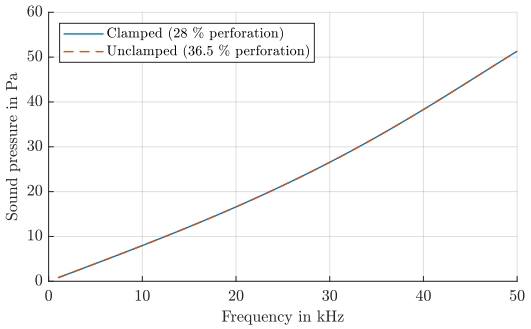

Figure 2: Comparison of the influence in the acoustic simulation using 28 %- or 36.5 % perforation grade for the bottom back plate. The back volume for this case has been defined by $d_\mathrm{BV} = 0.9$ mm and $h_\mathrm{BV} = 0.2$ mm.

For the computations an axi-symmetric Trelis model has been used to reduce the computational effort by only considering $1/12^\mathrm{th}$ of the overall valve. The model used for one exemplary computation can be seen in Fig. 3.

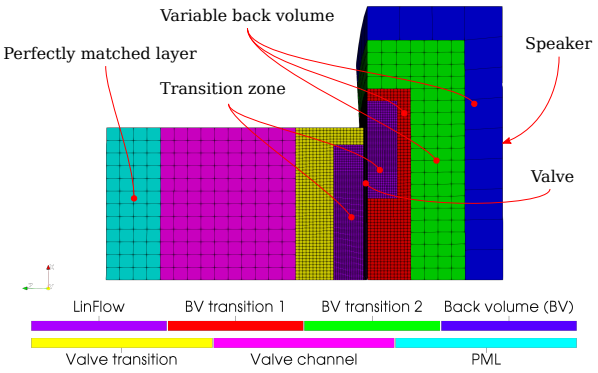

Figure 3: Exemplary mesh for a excitation frequency range of 10 kHz-20 kHz ($d_\mathrm{BV} = 0.9$ mm; $h_\mathrm{BV} = 0.2$ mm).

For the absorption of the outgoing waves a perfectly matched layer (PML) has been used. Regarding the coupling of the acoustic wave equation to the LF-equations as well as the coupling between differently meshed acoustic regions, non-conforming interfaces (NCI) have been utilized. The NCIs in the acoustic region have been solely used to reduce the computational effort by allowing for very quick transitions in element size while maintaining a structured mesh. This is especially important for the larger values of the back volume since the element sizes differ almost two orders of magnitude. The values for the size of the back volume are based on investigations with a hybrid demonstrator which has been investigated experimentally. The valve itself has been fully resolved as shown in Fig. 4 and consists of about 4×10^6 nodes for the LF-region as well as 1×10^5 nodes for the acoustic regions.

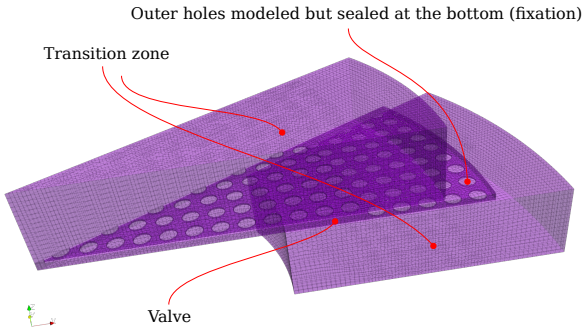

Figure 4: Close up of the valve and the surrounding transition zones.

Since we investigated a large frequency range, we inherently face the requirement of large transition zones as well as small elements for the correct development of the propagating wave [6]. The reason for this is given by

$$d_{\text{trans}} \geq 2\delta_{\text{visc}}(f_{\text{min}}) \tag{8}$$

and

$$h_{\text{el}} \leq \frac{\delta_{\text{visc}}(f_{\text{max}})}{10}, \tag{9}$$

with δ_{visc} given by

$$\delta_{\text{visc}}(f) = \sqrt{\frac{\mu}{\pi f \rho_0}} \tag{10}$$

as shown in [7]. Here d_{trans} represents the added length of an additional volume used for fading out the LF-domain. Furthermore, $\delta_{\text{visc}}(f)$ denotes the viscous boundary layer depending on the excitation frequency f, where f_{min} is used for the lowest considered frequency and f_{max} for the highest one. Finally, h_{el} stands for the maximum element size applicable to resolve all effects in the linearized flow region. In order to incorporate the requirements stated by (8) and (9), we used a dynamic transition zone characterized by d_{trans} which is adapted for different frequency ranges. Since the element size also has to be adapted, this leads to high RAM consumption. To reduce this computational effort, only about six elements per boundary layer can be ensured in the transition zone – inside the valve at least eight elements have been used. This leads to about 550 GB of RAM used for the largest computations.

Numerical computations

In order to study the influence of the back volume, a parameter study based on the ranges for the back volume given in Tab. 1 has been carried out with the help of our in-house open source FEM-solver `openCFS` [5]. Initially, a pure acoustic investigation has been performed in order to learn more about the system behaviour. Since we are dealing with MEMS structures with very narrow slits, a pure acoustic simulation is not enough, hence, the linearized flow equations have been used to perform an in-depth study in a second step.

Results for the acoustic wave equation

The results for the acoustic simulations including a close up for larger back volumes can be seen in Fig. 5 and are evaluated at a microphone position 250 µm above the BBP of the valve.

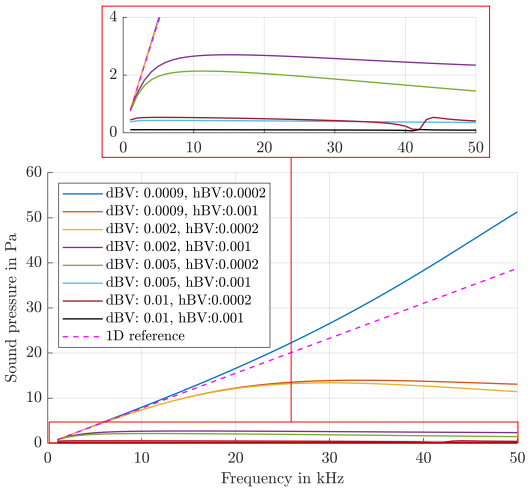

Figure 5: Results for the acoustic parameter study. A 1D-reference assuming plane waves has been used to show the convergence in the low frequency domain and to illustrate the deviation from it.

As it can be seen, a larger volume between the speaker and the valve worsens the transmission properties. The larger the back volume, the lower the frequency where the deviation from the reference starts. Furthermore, the effect of increasing the diameter or the height of the back volume is similar for both cases. Comparing the wave length to the size of the back volume suggests that the bump in the dark red line is most likely caused by a resonance effect.

Results for the linearized flow equations

Since the investigated valve is based on MEMS technology featuring slits in the µm region, the solution of the acoustic wave equation can be only seen as a rough estimation of the overall behaviour. In order to get reliable values for the actual sound pressure, viscous effects have to be included. As it can be seen from the results for the simulations using the linearized flow equations given in Fig. 6, these viscous effects have a strong influence on the transmission properties.

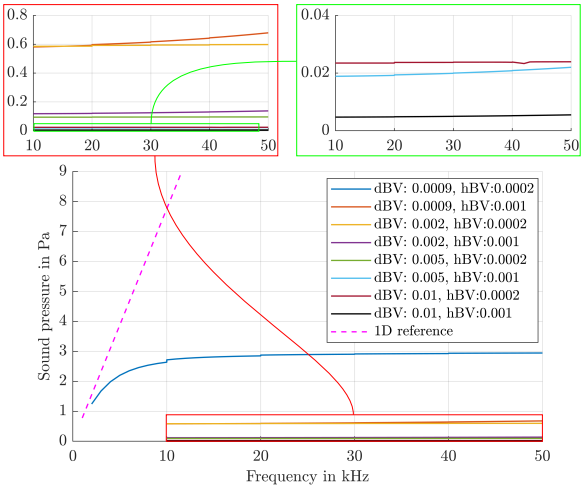

Figure 6: Results for the parameter study using the linearized flow equations. A 1D-reference assuming plane waves has been used to show the convergence in the low frequency domain and to illustrate the deviation from it. The discontinuities in the graphs are caused by the usage of different meshes for the same frequency.

In general, the acoustic sound pressure in the outlet is strongly reduced due to viscous effects. Again, the results converge for lower frequencies towards the linear reference. Here, only the best case based on the acoustic simulations has been evaluated down to 1 kHz. The reason for this is the use case for the valve. Since the investigation is for its usability for ADSR where pulses of small periods should be used, the lower frequency limit is not as interesting. Similar to the acoustic simulations, the effect of increasing the diameter or the height is relatively equal. Also, the bump in the dark red line is still visible but reduced in its amplitude due to the additional damping. Finally, discontinuities can be seen throughout the investigated frequency range. These are the direct result of the usage of different meshes for different frequency ranges. We have simulated the overlapping frequencies with both meshes in order to verify the mesh. Since the error is smaller than three percent for all cases, it can be stated, that the boundary layer is sufficiently resolved. Additionally, the error reduces for higher frequency ranges since the boundary layer scales with $1/\sqrt{f}$. Hence, the meshes tend to differ less for higher frequencies using equidistant frequency intervals.

Design guidelines

Based on the simulation results, general design guidelines can be proposed. Regarding the design of the volume between the speaker and the shutter it can be stated that a smaller back volume leads to multiple benefits. First of all, the simulations have shown that the sound transmission itself is improved. Furthermore, a smaller back volume also leads to increased resonance frequencies which reduces possible problems regarding the choice of the excitation frequency. Finally, the required form factor is ideal for MEMS applications due to their inherently small form factors.

Regarding the valve it has been seen that viscous effects can strongly limit the possible sound transmission. Hence, a small transmission impedance in the opened state is very important. Besides the disadvantage that the transmission in the opened state might suffer, viscous effects can also be used advantageous. Since they can reduce the sound transmission quite effectively, viscous effects can be used for sealing while avoiding a possible contact problem which would generate additional noise.

Conclusion

Based on numerical computations the basic actuator design for a new method of sound generation – called Advanced Digital Sound Reconstruction (ADSR) – was investigated. Therefore, a certain embodiment has been chosen and analyzed in a parameter study using the acoustic wave equation as well as the linearized flow equations. Due to the large frequency range investigated, an adaptive mesh has been used to generate reliable results. It has been shown that because of the small scale of the model, viscous effects need to be taken into account. Based on these results we have presented general guidelines on the design of the actuator for ADSR. These guidelines state that a small volume between the speaker and the shutter is essential for proper sound transmission. Furthermore, the viscous effects pose a challenge but also an opportunity regarding actuator design: While they can hinder sound transmission in the open state of the shutter, they can also be used for sealing purposes in the closed state. Hence, a fine tuning of the actuator to get the most beneficial design is essential.

References

[1] B. M. Diamond, J. J. Neumann, K. J. Gabriel: Digital sound reconstruction using arrays of CMOS-MEMS microspeakers. Fifteenth IEEE International Conference on Micro Electro Mechanical Systems (2002), pp. 292-295

[2] D. Mayrhofer and M. Kaltenbacher: Investigation of a new method for sound generation – Advanced Digital Sound Reconstruction. Proceedings of the German Annual Conference on Acoustics (DAGA) (Hannover, Germany, 2020), pp. 615-618.

[3] D. Mayrhofer and M. Kaltenbacher: Investigation of a new method for sound generation – Advanced Digital Sound Reconstruction. e & i Elektrotechnik und Informationstechnik 138 (2021), pp. 148–154.

[4] J. Manz, W. Klein and D. Tumpold: Photoacoustic Sensor Valve. U.S. Patent and Trademark Ofice, U.S. Patent Application No. 20200319144 (2020)

[5] M. Kaltenbacher: openCFS. `https://www.opencfs.org`, ver. 20.08 (2020)

[6] M. J. Cops, J. G. McDaniel, E. A. Magliula, D. J. Bamford: Analysis of thermal viscous boundary layers in acoustic absorption by metallic foam. The Journal of the Acoustical Society of America (2019)

[7] L. Gerlach: Thermoviskose Grenzschichteffekte (Schallführung in sehr engen Kanälen). Internal Fraunhofer IDMT report, unpublished (2018)